Impedance Spectroscopy for Enhanced Data Collection of Conductometric Soot Sensors

Middelburg, L.M.; Ghaderi, Mohammadamir; Bilby, David ; Visser, J.H.; Zhang, Kouchi; Wolffenbuttel, R.F.

DOI
10.1109/ISIE45063.2020.9152484

Publication date
2020

Document Version
Accepted author manuscript

Published in
2020 IEEE 29th International Symposium on Industrial Electronics (ISIE)

Impedance Spectroscopy for Enhanced Data Collection of Conductometric Soot Sensors

1st L.M. Middelburg
Department of Microelectronics
Delft University of Technology
Delft, the Netherlands
L.M.Middelburg@tudelft.nl

2nd M. Ghaderi
Department of Microtechnology and Nanoscience
Chalmers University of Technology
Chalmers, Sweden
mohammadamir.ghaderi@chalmers.se

3rd D. Bilby
Research and Advanced Engineering
Ford Motor Company
Dearborn, USA
dbilby@ford.com

4th J.H. Visser
Research and Advanced Engineering
Ford Motor Company
Dearborn, USA
jvisser@ford.com

5th G.Q. Zhang
Department of Microelectronics
Delft University of Technology
Delft, the Netherlands
G.Q.Zhang@tudelft.nl

6th R.F. Wolffenbuttel
Department of Microtechnology and Nanoscience
Chalmers University of Technology
Chalmers, Sweden
R.F.Wolffenbuttel@tudelft.nl

***Abstract*—Impedance spectroscopy in the frequency range 100 Hz to 10 kHz has been applied to the Inter-Digitated Electrode (IDE) structure that is conventionally operated as a resistive sensor for the measurement of Particulate Matter (PM). The measurement of both the in-phase (resistive) and out-of-phase (capacitive) components of the impedance over this frequency range provides more data on PM as compared to DC resistance measurement only. Experimental validation confirms a more gradual change in capacitance with soot buildup as compared to the sudden reduction of resistance with dendrite formation. The effect of an additional vertical electric field for an increased capacitive sensitivity due to stimulated soot build-up has been experimentally investigated using the electrically conductive flow housing of the IDE structure as an additional suspended electrode.**

***Index Terms*—Particulate matter sensing, impedance spectroscopy, resistive soot sensor, exhaust gas after-treatment, on-board diagnostics**

I. Introduction

Automotive emissions have an impact on health and the environment, which has resulted in regulations in the form of standards on acceptable maximum emissions [1]–[4].

Compliance requires amongst others particulate filters in the exhaust after-treatment. For diesel powertrains this so-called Diesel Particulate Filter (DPF) may need to be diagnosed for leaks. The current requirements in Europe and North-America necessitate the use of a PM sensor downstream of the DPF [5].

The commonly used sensor for DPF leakage monitoring is referred to as the resistive soot sensor or conductometric soot sensor. This sensor consists of two Inter-Digitated Electrodes (IDEs, the combination is sometimes referred to as an Inter-Digitated Transducer IDT, or Finger Electrode Structure - FES), which are biased at approximately 45 V_{DC} [6]. Upon exposure to a soot containing gas flowing over the sensor surface, soot particles are deposited on the sensor surface by a combination of thermophoretic and electrophoretic forces [7]. The soot deposits in the form of dendrites that bridge the electrodes and form conductive paths. In the usual implementation the change in resistance is detected. There have been reports on the effect of electrophoresis in an IDE when combined with capacitive readout [8]. Moreover, when Joule heating of the dendrites themselves is considered, the voltage bias on an IDE structure should be limited to ensure optimal soot response time [9]. The disadvantage of this implementation is the long response time (dead time) until a conducting path is formed and a detectable current signal, that indicates a DPF leak, becomes available. This undesired property is even more of concern when the smaller particles are considered, which have a relative minor contribution to the build-up of the conductive path [10]. It should be noted that the measurement technique is limited to the real part of the impedance only (i.e. only the resistivity is measured at a DC voltage).

The time it takes for diagnosing a leaky DPF at a given soot concentration is highly important to actual compliance with emission requirements and is a critical performance parameter [11]. Several attempts for reducing response time of resistive PM sensors have been reported. The main approach involves optimization of applied bias [12]. Increased bias leads to increased electrostatic soot capture and therefore faster response. However, the voltage limitation to prevent the destruction of the dendrites by Joule heating mentioned already does apply [7]. Response time reductions have also been investigated through application of small device modifications and alternative measurement modes, such as capacitance [13] and parallel resistance [14]. The approach presented here is basically a generalization of these measurement modes in combination with the use of an AC voltage. Measuring the full impedance of the IDE could provide the additional information for an improved sensitivity of PM or a reduced response time.

Electrophoretic effects have been reported to provide current amplification by Bilby et al. [15]. The effect is occurring in an additional vertical electrode arrangement biased at a high

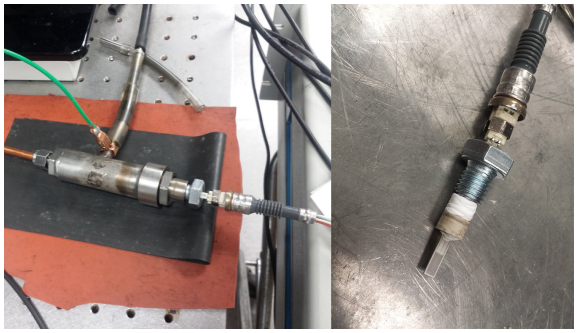

Fig. 1. The sensor within its flow housing. Note the high voltage (HV) connection to the housing and the isolating pad (left). The ceramic IDE structure along with its mountable holder (right).

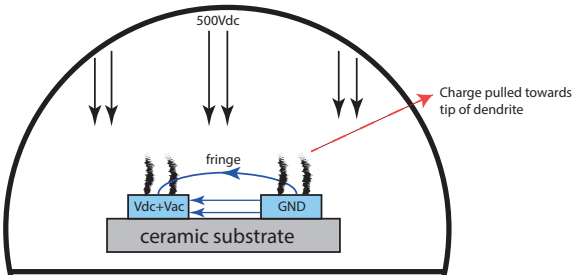

Fig. 2. A schematic overview of the cross section of the measurement cell explaining the motion of the isolated charge in the fringing E-field across the IDE structures.

voltage (HV). The vertical electric field causes dendrites to grow in the vertical direction and affects the dendrites which could lead to polarization effects, potentially increasing the electrical capacitance and is considered here as an additional option for controlling sensor response. Therefore, in this work impedance spectroscopy over a broad frequency range is applied to a resistive IDE based soot sensor to investigate what improvements can be made to state-of-the art particle sensing.

The organization of the paper is as follows. After the presentation of the basic IDE structure, the modeling is described, which would enable the interpretation of the impedance measurements. This modeling is validated in Section III using results of impedance spectroscopy at different settings of the lateral and vertical components of the electric fields. Finally, conclusions are drawn in Section IV.

II. Model Derivation

In this section the interaction between the particle-containing gas flow and the sensor structure is modeled. The structure used in this work is a modified version from a commercially available resistive soot sensor with IDE fingers. The bare substrate with the IDE's is put in a custom-made flow housing to which an optional high voltage can be applied, yielding a vertical electrical field with respect to the surface of the substrate. This vertical electrical field is intended to verify the effect on capacitive soot sensitivity. Images of the used sensor are included in Fig. 1, including the assembled structure with flow housing to which a high-voltage can be applied for generating a controllable vertical electric field. A more schematic representation of the sensor structure and flow housing is shown in Fig. 2. As can be noted, there are two different electrical fields: a lateral field between the IDE fingers and a vertical electrical field with respect to the electrodes introduced by the high voltage, applied to the housing. For simplicity both field are drawn orthogonally. To investigate the behavior of soot deposition and deposited dendrites as function of the orthogonal electric field, the magnitude of both fields can be varied. In addition, the IDE structures can be excited with both DC bias voltages as well as AC sinusoidal voltages by using an impedance analyzer.

The simple equivalent circuit model considered for modeling is a parallel resistor and capacitor, where the resistor is a lumped element representing the distributed resistivity between the electrodes, while the parallel capacitor is a lumped element representing the distributed capacitance between the electrodes. It should be noted that models based on quantized, kinetic descriptions of dendrite growth, such as those in [15] and [16] are available for predicting the dynamic behavior of resistive PM sensors. Nevertheless, the simple RC-section is chosen here, because it allows a description of the sensor performance in electrical parameters. The raw impedance data $|Z|$ and θ is mapped on this equivalent circuit and can be used to evaluate which component is more suitable for measuring deposited soot. The proposition explored here is that the physical mechanisms of the changes in IDE resistance and capacitance are different in nature. The increased capacitance over time is assumed to result from gradual vertical dendrite growth on top of the electrodes, while the resistance is reduced by dendrites which are growing in-plane in the lateral direction. The change of these two passive elements over time can be used for indirect experimental validation of the proposition.

1) Parallel resistance: The parallel resistance is determined by the grown soot dendrites between both IDE's. Each dendrite crossing the IDEs can be considered as a resistance much smaller than the air bulk resistivity. Although the resistance of each crossing dendrite is different, one could state that the resistance can be described in terms of statistical parameters and there would be an average dendrite-bridge resistance R_o.

After the first bridge results $R = R_o$ and after the second bridge formed in $R = \frac{Ro}{2}$.

During deposition, these resistive bridges are continuously formed, resulting in an increasing number of equal-value resistors in parallel, thus a linearly increasing conductance. For a large number of bridges and a constant interval between subsequent bridges, the change of total measured parallel resistance R is described by the following equation.

$$R_{eq} = \frac{R_0}{n} \tag{1}$$

Where R_{eq} is equal to the equivalent measured resistance, R_0 to the average dendrite-bridge resistance and n to the number of dendrites.

2) Parallel capacitance: Soot particles flowing over the flow housing that contains the substrate with the IDE structure are subject to several forces, such as thermophoretic forces and gravitational forces, but also to electrostatic forces. As a result, a proportion is deposited on the sensor surface and contributes to the growth of dendrites in a direction that is, amongst others, influenced by the local electric field. With the dendrites being on top of the IDE electrodes, the tip of the dendrites are assumed flexible and can move in the varying fringing electrical field lines of the lateral electrical field, caused by the AC excitation on the IDE. By doing so, the charge is moving in the electrical field, thus contributing to the relative permittivity, thereby increasing the measured parallel capacitance. The growth and movement of the soot agglomerate and dendrites increases the relative permittivity. To calculate the effect of the dendrites on the ϵ_r the polarization P needs to be determined.

$$P = \frac{dp}{dV} = \frac{dq \cdot x}{dV} \tag{2}$$

Here dV stands for the volume portion of the airspace over the sensor, including the dendrite, carrying a charge of dq. As the dendrites bend due to the time-varying local electric field because of the AC excitation, the dV section moves by x in the fringing fields of the electric field across the IDE fingers.

$$dq = N \cdot dV \cdot q_{avg} \tag{3}$$

Where N represents the number of the grown dendrites on top of the IDE fingers and q_{avg} represents the amount of charge per soot dendrite. The displacement of the dendrite, and its dV section, is due to electric force and depends on its mechanical rigidity, which can be expressed as an effective stiffness K_{eff}.

$$F_E = qE = K_{eff}x \tag{4}$$

Substituting the equations above the polarization becomes:

$$P = Nq_{avg}x = \frac{Nq_{avg}^2 E}{K_{eff}} \tag{5}$$

The resulting relative permittivity can be calculated from electric displacement.

$$D = \epsilon_0 E + P = \epsilon_r \epsilon_0 E \tag{6}$$

$$\epsilon_r = 1 + \frac{Nq_{avg}^2}{\epsilon_0 K_{eff}} \tag{7}$$

The relative permittivity increases with the number of the dendrites growing over the IDE and the square of the average charge of the dendrites. This increase in effective permittivity results in a measurable increase in the IDEs capacitance.

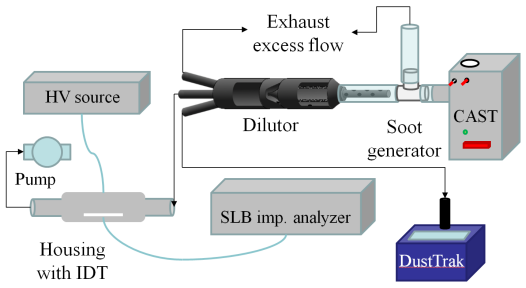

Fig. 3. A schematic overview of the measurement setup.

TABLE I
OVERVIEW OF THE DIFFERENT E-FIELDS ON AND AROUND THE SENSOR ELEMENT.

V	Amplitude [V]	Field	Gap	E-field [V m^{-1}]
AC	3	horizontal	45 μm	6.67×10^4
HV	500	vertical	2.5 mm	2×10^5

III. EXPERIMENTAL

The measurement setup used consists of a Jing 5201c miniCAST soot generator, a diluter with variable dilution ratio, the measurement cell itself and a Schlumberger SI1260 impedance analyzer to measure the impedance of the soot sensor. A Stanford Research Systems PS365 high voltage power supply is connected to the sensor flow housing. A commercially available soot sensor consisting of an IDE transducer on a ceramic substrate was modified to alter the soot-containing aerosol flow. A custom flow housing has been fabricated by welding stainless steel, in which the modified soot sensor was installed (see also Figure 1). The diluter is used to dilute the soot-rich gas stream from the CAST to yield a soot concentration which is representative of real exhaust gas. Flow through the sensor housing is controlled with an air pump, control valve and is calibrated using a flow meter. An approximate flow rate of 500 cm^3 min^{-1} was used throughout the measurements. The setting of the soot generator was such that the mean particle diameter equals 80 nm. The CAST, the diluter and the impedance analyzer are controlled and read-out by a LabView program running on a PC. The raw impedance data (magnitude and phase) is mapped on the equivalent model parameters, c.q. parallel capacitance and resistance. A schematic overview of the measurement setup is included in Fig. 3.

Transient soot deposition measurements were carried out, while simultaneously measuring the impedance of the IDE using an impedance analyzer. The impedance was measured over the range 100 Hz to 10 kHz. Only the sub-range 700 Hz to 10 kHz proved useful, because of the effects of noise and parasitic components at lower frequencies, which have not been considered in the simple modeling. Transient soot deposition measurements have been carried out at the two orthogonal electrical fields as summarized in Table I. AC voltage excitation with magnitude of 3 V on the IDE, with the housing at 500 V_{DC}, resulting in an electrical field with

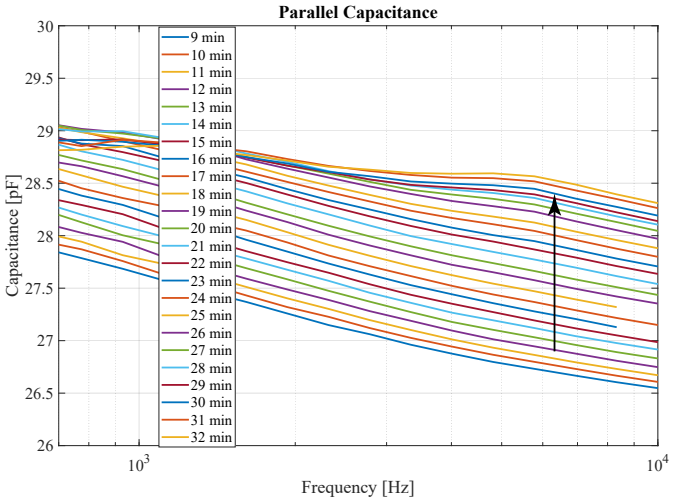

Fig. 4. The measured parallel capacitance of the transient soot deposition experiment, derived from raw impedance data mapped on a parallel RC network. The arrow indicates the direction of proceeding time. Note the constant and linear increase of the parallel capacitance for fixed time intervals.

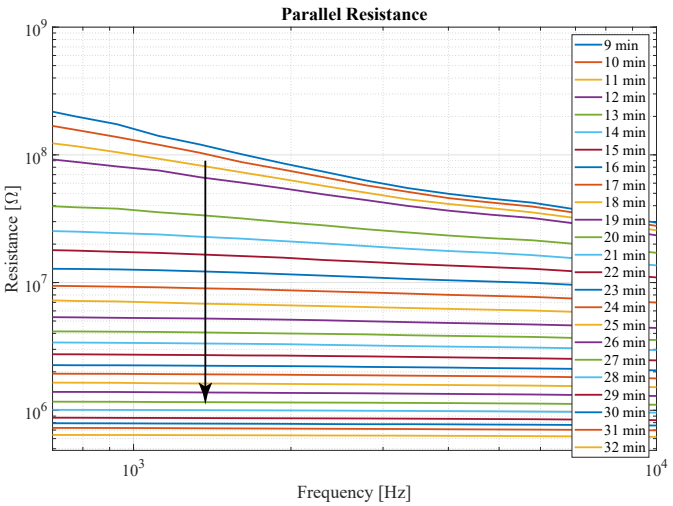

Fig. 5. The measured parallel resistance of the transient soot deposition experiment, derived from raw impedance data mapped on a parallel RC network. The arrow indicates the direction of proceeding time. Note the exponential behavior on the logarithmic y-axis of the parallel resistance for fixed time intervals. It should also be noted that for the first measured traces (9-12 minutes) the resistance is decreasing with increasing frequency, due to proceeding measurement time while the frequency vector is measured by the impedance analyzer.

an approximated magnitude of $2 \times 10^5\,\mathrm{V\,m^{-1}}$ in the vertical direction and $6.67 \times 10^4\,\mathrm{V\,m^{-1}}$ in horizontal direction. The parallel capacitance and resistance are included in Figs. 4 and 5.

Our measurements indicate that the capacitance changes starting from the fourth minute and increases more gradual with soot buildup as compared to the sudden reduction of resistance with dendrite formation at the eighth minute. It remains to be investigated whether these time dependencies are sufficiently significant and repeatable for accurate characterization of a DPF leak level. Measurements at variable vertical field reveal a higher capacitive sensitivity with increased vertical electric field strengths. Moreover, the response time at a given soot exposure is reduced. These are preliminary dead time results that need to be investigated in more detail. We expect the bending of dendrites by the electric field to contribute to this effect.

IV. Conclusion

Impedance spectroscopy has been applied to an IDE structure on a ceramic substrate, with an out-of-plane additional electrode to enable the application of a vertical E-field. Several combinations of horizontal and vertical E-fields are applied by electrically biasing the IDE and out-of-plane electrode, and the influence on deposited soot dendrites is studied. Approximate analytical expressions were derived and have resulted in an equivalent circuit model.

The raw impedance data supports the equivalent circuit model of a parallel capacitor and resistor. In all cases was an increasing capacitance observed with a vertical electrical field.

In general it can be concluded that the capacitance increases in a gradual way, in contrast to the rather sudden reduction of the parallel resistance value caused by dendrite formation. The exponential signal shape of the resistance, along with stochastic noise in dendrite growth, is typically undesired for accurate characterization of a DPF leak level, as the sensor is then treated as a switch rather than delivering a quantitative sensor signal. Whether or not the capacitance increases, depends on the magnitude of the vertical E-field compared to the magnitude of the lateral E-field, a larger vertical field is demonstrated to be advantageous. It remains to be investigated whether the observed effects are sufficiently pronounced and repeatable for practical use.

Future work includes investigation of Micro-Electro Mechanical System (MEMS) technology for the fabrication of more repeatable cells, where the opposing electrodes both consists of an IDE. Additionally, the effect of spacing between the IDE fingers and the relative position of both sets of IDEs can be investigated.

References

[1] P. Karjalainen, L. Pirjola, J. Heikkil, T. Lhde, T. Tzamkiozis, L. Ntziachristos, J. Keskinen, and T. Rnkk, "Exhaust particles of modern gasoline vehicles: A laboratory and an on-road study," *Atmospheric Environment*, vol. 97, pp. 262–270, 2014. [Online]. Available: http://www.sciencedirect.com/science/article/pii/S1352231014006190

[2] D. Lutic, J. Pagels, R. Bjorklund, P. Josza, J. H. Visser, A. W. Grant, M. L. Johansson, J. Paaso, P.-E. Fgerman, and M. Sanati, "Detection of soot using a resistivity sensor device employing thermophoretic particle deposition," *Journal of sensors*, vol. 2010, 2010.

[3] F. Forastiere, "Fine particles and lung cancer," 2004.

[4] J. S. Patton and P. R. Byron, "Inhaling medicines: delivering drugs to the body through the lungs," *Nature reviews Drug discovery*, vol. 6, no. 1, p. 67, 2007.

[5] T. Kamimoto, "A review of soot sensors considered for on-board diagnostics application," *International Journal of Engine Research*, vol. 18, no. 5-6, pp. 631–641, 2017.

[6] A. Malik, H. Abdulhamid, J. Pagels, J. Rissler, M. Lindskog, P. Nilsson, R. Bjorklund, P. Jozsa, J. Visser, A. Spetz *et al.*, "A potential soot mass

determination method from resistivity measurement of thermophoretically deposited soot," *Aerosol Science and Technology*, vol. 45, no. 2, pp. 284–294, 2011.

[7] G. Hagen, C. Spannbauer, M. Feulner, J. Kita, A. Müller, and R. Moos, "Conductometric soot sensors: Internally caused thermophoresis as an important undesired side effect," *Sensors*, vol. 18, no. 10, p. 3531, 2018.

[8] G. Hagen, M. Feulner, R. Werner, M. Schubert, A. Müller, G. Rieß, D. Brüggemann, and R. Moos, "Capacitive soot sensor for diesel exhausts," *Sensors and Actuators B: Chemical*, vol. 236, pp. 1020–1027, 2016.

[9] D. Grondin, P. Breuil, J. P. Viricelle, and P. Vernoux, "Modeling of the signal of a resistive soot sensor, influence of the soot nature and of the polarization voltage," *Sensors and Actuators B: Chemical*, vol. 298, p. 126820, 2019. [Online]. Available: http://www.sciencedirect.com/science/article/pii/S0925400519310196

[10] A. Reynaud, M. Leblanc, S. Zinola, P. Breuil, and J.-P. Viricelle, "Responses of a resistive soot sensor to different mono-disperse soot aerosols," *Sensors (Basel, Switzerland)*, vol. 19, no. 3, p. 705, 2019. [Online]. Available: https://www.ncbi.nlm.nih.gov/pubmed/30744083 https://www.ncbi.nlm.nih.gov/pmc/articles/PMC6387397/

[11] S. Binnig, S. Fuchs, C. R. Collantes, and H.-R. Volpp, "Exhaust gas condensate–formation, characterization and influence on platinum measuring electrodes in diesel vehicles," *Sensors and Actuators B: Chemical*, vol. 242, pp. 1251–1258, 2017.

[12] D. Grondin, A. Westermann, P. Breuil, J. P. Viricelle, and P. Vernoux, "Influence of key parameters on the response of a resistive soot sensor," *Sensors and Actuators B: Chemical*, vol. 236, pp. 1036–1043, 2016. [Online]. Available: http://www.sciencedirect.com/science/article/pii/S0925400516307250

[13] G. Hagen, G. Riess, M. Schubert, M. Feulner, A. Müller, D. Brüggemann, and R. Moos, "Capacitive soot sensor," *Procedia engineering*, vol. 120, pp. 241–244, 2015.

[14] P. Bartscherer and R. Moos, "Improvement of the sensitivity of a conductometric soot sensor by adding a conductive cover layer," *J. Sens. Sens. Syst*, vol. 2, pp. 95–102, 2013.

[15] D. Bilby, D. J. Kubinski, and M. M. Maricq, "Current amplification in an electrostatic trap by soot dendrite growth and fragmentation: Application to soot sensors," *Journal of Aerosol Science*, vol. 98, pp. 41–58, 2016. [Online]. Available: http://www.sciencedirect.com/science/article/pii/S002185021530104X

[16] D. Grondin, P. Breuil, J. P. Viricelle, and P. Vernoux, "Modeling of the signal of a resistive soot sensor, influence of the soot nature and of the polarization voltage," *Sensors and Actuators B: Chemical*, vol. 298, p. 126820, 2019. [Online]. Available: http://www.sciencedirect.com/science/article/pii/S0925400519310196